Journal of Statistical Physics, Vol. 81, Nos. 1/2, 1995

Heat Transfer in Lattice BGK Modeled Fluid

Y. Chen,[1] H. Ohashi,[1] and M. Akiyama[1]

Received September 7, 1994; final February 27, 1995

The thermal lattice BGK model is a recently suggested numerical tool aiming at solving problems of thermohydrodynamics. The quality of the lattice BGK simulation is checked in this paper by calculating temperature profiles in the Couette flow under different Eckert and Mach numbers. A revised lower order model is proposed to improve the accuracy and the higher order model is proved to be advantageous in this respect, especially in the flow regime with a higher Mach number.

KEY WORDS: Lattice Boltzmann; BGK approximation; heat transfer; computational fluid dynamics; transonic flow.

1. INTRODUCTION

The lattice BGK method can be viewed as the latest development of the lattice Boltzmann (LB) method,[2] which is a derivation of the lattice gas automata (LGA) model[1] for the simulation of fluid dynamics. Such a development was achieved by introducing the simple Bhatnagar–Gross–Krook collision operator[6] into the lattice Boltzmann equation (LBE).[3-5] Although this single-time-relaxation approximation (STRA) made on the collision term of the discrete kinetic equation looks oversimplified, lattice BGK models amazingly reproduce the complexities of fluid flows. This has been the subject of several studies.[7-9]

Recently, lattice BGK models in which thermal effects are included were explored by a number of authors.[10, 11, 13, 15] These models are established by dealing with the conservation of particle kinetic energy non-trivially, a treatment which can be realized with the use of multispeed particle distributions. The employment of a composed lattice is basically

[1] Department of Quantum Engineering and Systems Science, Faculty of Engineering, University of Tokyo, Tokyo, Japan.

0022-4715/95/1000-0071$07.50/0

required. Here, the composed lattice is defined as a lattice consisting of several sublattices whose link vectors have different moduli and/or different spatial rotations. For instance, Alexander *et al.*[10] employed a composed hexagonal lattice in two-dimensional space which contains two hexagonal sublattices with one and two moduli and identical rotations for the link vectors. Others used the composed square lattice in D-dimensional space; see Fig. 3 for a 2D example. One may further divide those thermal lattice BGK models, within a parametrized equilibrium framework, into two classes: the lower order models (models of Alexander *et al.*[10] and Qian and Orszag[11]) and the higher order model (model of Chen *et al.*[13]). The word "order" here refers to the order of the flow speed u in its expansion of the equilibrium particle distribution. The lattice kinetic equation used in all the numerical simulations with these models is

$$N_{pki}(\mathbf{x}+\mathbf{c}_{pki}, t+1) - N_{pki}(\mathbf{x}, t) = -\frac{1}{\tau}(N_{pki} - N_{pki}^{[\mathrm{eq}]}) \tag{1}$$

Here, N_{pki} denotes the particle distribution on the ith link of the pk sublattice; $\mathbf{c}_{pki}$ is the link vector and therefore the vector of the particle flight velocity. The r.h.s. of Eq. (1) indicates the use of STRA, and τ is the relaxation time period during which particle distributions approach equilibrium values. With the exception of McNamara and Alder's study,[15] in which the authors followed a formulation similar to the moment expansion method to decide the equilibrium particle distribution, $N_{pki}^{[\mathrm{eq}]}$ is usually written in the low-speed expansion up to the second (or third) order of u for the lower order models and fourth order for the higher order model. Correspondingly, lattice symmetries of various levels are required for these models, in order that the momentum and heat flux tensors can be expressed in an isotropic form in the macroscopic limit. Specifically, the nth-rank particle velocity-moment tensor defined as

$$T_{pk\alpha\ldots\xi}^{(n)} = \sum_i \overbrace{c_{pki\alpha}\cdots c_{pki\xi}}^{n \text{ components}} \tag{2}$$

is required to have an isotropic form up to $n=4$ for the lower order models and $n=6$ for the higher order model. The latter would prevent one from using the composed hexagonal lattice in 2D space and the FCHC lattice in 4D space, for that the highest rank of the isotropic velocity-moment tensor is four in both cases.[14]

The higher order model is more accurate, which was demonstrated by the numerical measurement of decaying rates of the flow kinetic energy under different Mach numbers.[13] In that case, the higher order model was

shown to be free from the deviations caused by the nonlinear terms hidden in the r.h.s. of the momentum equation of the modeled fluid. The purpose of this study is devoted, however, to the modeling of heat transfer with the thermal lattice BGK models. The investigation was carried out by measuring and comparing the temperature profiles in the Couette flows under different Eckert numbers and Mach numbers. Models based on the composed square lattice were used in all these calculations. Key issues of the thermal lattice BGK model will be briefly reviewed in the next section, and numerical experiments and their results will be described subsequently. The lower and higher order models used in this paper will be labeled as follows:

- 2D13VQ: Qian's lower order model, based on the 2D 13-link composed square lattice.
- 2D13VC: A revised lower order model, based on the 2D 13-link composed square lattice.
- 2D16V: Chen's higher order model, based on the 2D 16-link composed square lattice.

Discussions are confined to two-dimensional cases. Some concluding remarks are given in the last section.

2. THERMAL LATTICE BGK MODELS

2.1. Coordinates and Symmetries of the Composed Lattice

The coordinates of link vectors of the square sublattices may be written,

$$k(\overbrace{\underbrace{\pm 1, \pm 1, \ldots, \pm 1}_{p \text{ components}}, 0, \ldots, 0, 0}^{D \text{ components in } D \text{ dimensions}}) \tag{3}$$

and permutations of this expression. Here, the number of nonzero components is p, so that the modulus of such a vector is $|\mathbf{c}_{pki}| = k\sqrt{p}$. It is important to know, in the process of hydrodynamic derivation, the structure of the velocity-moment tensor $T^{(n)}_{pk\alpha\ldots\xi}$, which consists of the n-product of these link vectors. The odd-rank tensors vanish naturally by the definition [Eq. (2)] itself. The even-rank tensors, in particular second-, fourth-, and sixth-rank tensors, can be written in D-dimensional space,

$$\begin{aligned} T^{(2)}_{pk\alpha\beta} &= \vartheta_{pk}\delta_{\alpha\beta} \\ T^{(4)}_{pk\alpha\beta\gamma\delta} &= \psi_{pk}\Upsilon_{\alpha\beta\gamma\delta} + \varphi_{pk}(\delta_{\alpha\beta}\delta_{\gamma\delta} + \delta_{\alpha\gamma}\delta_{\beta\delta} + \delta_{\alpha\delta}\delta_{\beta\gamma}) \\ T^{(6)}_{pk\alpha\beta\gamma\delta\zeta\xi} &= \Lambda_{pk}\Upsilon_{\alpha\beta\gamma\delta\zeta\xi} + \Omega_{pk}(\delta_{\alpha\beta}\Upsilon_{\gamma\delta\zeta\xi} + \ldots) + \Theta_{pk}(\delta_{\alpha\beta}T^{(4)}_{pk\gamma\delta\zeta\xi} + \ldots) \end{aligned} \tag{4}$$

Here, δ is the Kronecker tensor and Υ is its higher order version, which, by definition, is 1 if all the subscripts are the same and 0 otherwise. The ellipses stand for terms which can be obtained by permuting the indices of the foregoing terms. Numerical values of parameters such as ϑ_{pk}, ψ_{pk},..., Θ_{pk} are listed[12, 13] for one, two, and three dimensions. The way to make the macroscopic flux tensors isotropic is to tune the particle populations on different sublattices properly so that the sum of anisotropic parts, parts that are related to ψ_{pk}, Λ_{pk}, and Ω_{pk}, vanishes as a total effect.

2.2. Equilibrium Particle Distribution

When the flow speed of the modeled fluid is controlled to be much smaller than the flight speed of particles, the local equilibrium particle distribution can be expanded around the uniform equilibrium state. In a lattice Boltzmann formulation, due to the flexibilities in residence and number of particles and the parity invariance of the square lattice, the low-speed expansion can be generically formulated as follows:

$$\begin{aligned} N_{pki}^{[eq]} = A_{pk} + M_{pk}(c_{pki\alpha}u_\alpha) + G_{pk}u^2 + J_{pk}(c_{pki\alpha}u_\alpha)^2 \\ + Q_{pk}(c_{pki\alpha}u_\alpha)\,u^2 + H_{pk}(c_{pki\alpha}u_\alpha)^3 \\ + R_{pk}(c_{pki\alpha}u_\alpha)^2u^2 + S_{pk}u^4 + \mathcal{O}(u^5) \end{aligned} \tag{5}$$

For the lower order models, terms whose orders are higher than u^2 may be cut off, or one of the third-order terms can be retained to make the energy equation more accurate on the Euler level.[12] Parameters of the expansion will depend on two of the locally conserved quantities, namely density ρ ($\equiv\sum_{pki}N_{pki}$) and thermal energy e ($\equiv\frac{1}{2}\sum_{pki}N_{pki}\,|c_{pki}-u|^2$). Furthermore, this dependence may be described in the form:

$$X_{pk} = \rho \sum_{l=0}^{2} x_{pkl}e^l \tag{6}$$

Here, X_{pk} may represent any one of A_{pk}, M_{pk},..., S_{pk}, so that x_{pkl} is actually a_{pkl}, m_{pkl},..., s_{pkl}. Various constraints are directly imposed on x_{pkl}, with which definitions of the conserved quantities can be justified, and the vanishing of the anisotropic parts of macroscopic flux tensors and the non-existence of unphysical artifacts in the macrodynamic equations can be ensured in the meantime. The number of such constraints is usually smaller than that of the parameters, so that the specification of a thermal lattice BGK model always involves some arbitrariness.[12, 15] This implies that some optional constraints may be employed either to minimize the higher

rank anisotropic effects or to improve the accuracy for the model, which will be made clear in the following text.

2.3. Macroscopic Flux Tensors and Transport Coefficients

In the hydrodynamic derivation process for the lattice BGK models, the lattice BGK equation, Eq. (1), is first Taylor expanded into a continuous form in the long-wavelength, low-frequency limit. Macrodynamic equations for the conserved quantities can be obtained subsequently by using the multiscale technique, which is a perturbative formulation method. The small quantity for the perturbation is chosen to be proportional to the local Knudsen number and is denoted as ε. Correct forms of the macrodynamic equations are guaranteed by correct expressions of the macroscopic flux tensors, which are again ensured by the aforementioned constraints imposed on the parameters of the low speed expansion of the equilibrium particle distribution. The resulting momentum flux tensors on the Euler (ε) order and Navier–Stokes (ε^2) order are

$$\Pi^{(0)}_{\alpha\beta} = \sum_{pki} N^{(0)}_{pki} c_{pki\alpha} c_{pki\beta} = \frac{2}{D} \rho e \delta_{\alpha\beta} + \rho u_\alpha u_\beta \tag{7}$$

$$\begin{aligned} \Pi^{(1)}_{\alpha\beta} &= \left(1 - \frac{1}{2\tau}\right) \sum_{pki} N^{(1)}_{pki} c_{pki\alpha} c_{pki\beta} \\ &= -\frac{2}{D} \rho e \left(\tau - \frac{1}{2}\right) \left[(\partial_\alpha u_\beta + \partial_\beta u_\alpha) - \frac{2}{D} (\partial_\gamma u_\gamma) \delta_{\alpha\beta} \right] \end{aligned} \tag{8}$$

Here $N^{(0)}_{pki}$ is the equilibrium and $N^{(1)}_{pki}$ is the nonequilibrium part of the particle distribution. Heat flux vectors on different orders may be expressed as

$$q^{(0)}_\alpha = \frac{1}{2} \sum_{pki} N^{(0)}_{pki} |c_{pki} - u|^2 (c_{pki\alpha} - u_\alpha) = 0 \tag{9}$$

$$\begin{aligned} q^{(1)}_\alpha &= \frac{1}{2} \left(1 - \frac{1}{2\tau}\right) \sum_{pki} N^{(1)}_{pki} |c_{pki} - u|^2 (c_{pki\alpha} - u_\alpha) \\ &= -\frac{2(D+2)}{D^2} \rho e \left(\tau - \frac{1}{2}\right) \partial_\alpha e \end{aligned} \tag{10}$$

Transport coefficients and the state equation of the modeled fluid can be easily identified from these formulas; for example, the shear viscosity and the heat conductivity read, respectively,

$$\mu = \frac{2}{D} \rho e \left(\tau - \frac{1}{2} \right) \tag{11}$$

$$\kappa = \frac{D+2}{D} \rho e \left(\tau - \frac{1}{2} \right) \tag{12}$$

Note that the accuracies of Eqs. (7)–(10) are different for models of different orders. For the lower order models, $\Pi^{(0)}_{\alpha\beta}$ and $q^{(0)}_{\alpha}$ are accurate up to εu^3 and εu^2 orders, and $\Pi^{(1)}_{\alpha\beta}$ and $q^{(1)}_{\alpha}$ up to $\varepsilon^2 u^2$ and $\varepsilon^2 u$ orders. For the higher order model, the accuracies of the corresponding quantities are upgraded to εu^5, εu^4, $\varepsilon^2 u^4$, and $\varepsilon^2 u^3$ orders.

3. NUMERICAL INVESTIGATIONS

3.1. Couette Flow

The flow system is an extremely simple one, consisting of one moving boundary, one boundary at rest, and the fluid layer in between (Fig. 1). In the case that the two parallel walls have identical temperatures, the dissipative work of the viscous force will still lead to a parabolic temperature distribution inside the fluid layer. This should serve as a good test case for checking the lattice BGK modeling of heat transfer, because the contribution of heat conduction is reduced, so that deviations in the viscous work would turn up if there were any. On the contrary, if the temperature gradient is too strong, deviations in the viscous work would be difficult to detect, as they are orders higher than the heat conduction term.

From the viewpoint of dimensional analysis, the heat transfer in such a system is governed by two dimensionless parameters, namely the Prandtl number and the Eckert number. As the Prandtl number of the lattice BGK

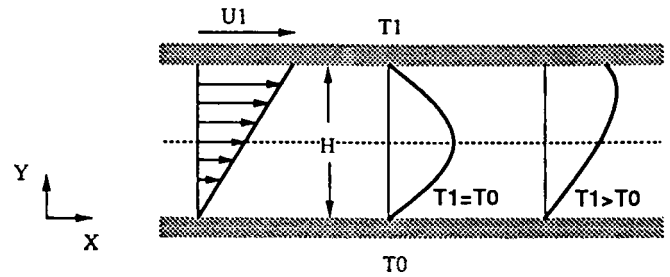

Fig. 1. Velocity and temperature distributions in Couette flow.

modeled fluid has an invariable unit value,[12, 15] the Eckert number, defined as

$$E=\frac{U_1^2}{c_p(T_1-T_0)} \tag{13}$$

becomes a decisive parameter. The definition of the Eckert number tells that it is a measure of the ratio between the heat due to friction and that due to conduction. Note that this number becomes infinite when viscous heating prevails, and is small when the heat conduction dominates. The analytical solution of the steady temperature distribution in the transverse direction of the channel can be obtained by directly solving the Navier–Stokes equations with the proper boundary conditions, which read

$$T_1 \neq T_0: \qquad T-T_0=\frac{y}{H}(T_1-T_0)+\frac{\mu U_1^2}{2\kappa}\frac{y}{H}\left(1-\frac{y}{H}\right) \tag{14}$$

$$T_1 = T_0: \qquad T-T_0=\frac{\mu U_1^2}{2\kappa}\frac{y}{H}\left(1-\frac{y}{H}\right) \tag{15}$$

Hence in the following calculations, numerical results will be normalized with (T_1-T_0) if $T_1 \neq T_0$ or with $\mu U_1^2/2\kappa$ otherwise. The linear distribution of the flow velocity will not be depicted here, as it can always be obtained as long as the steady stage of flow is reached.

3.2. Results of Qian's Model (2D13VQ)

The model used here is a typical lower order thermal lattice BGK model on the composed square lattice. Conditions for the numerical calculation are as follows: lattice size 64×32, time step 10,000, moving boundary at $y/H=1$, and non-slip and fixed-temperature boundary conditions. The analytical solutions and the numerical results are compared with each other in Fig. 2, from which one may conclude that the numerical calculation is accurate only when the Eckert number is small enough, that is, when the temperature distribution is mainly controlled by the heat conduction between the two walls. Notice that the Mach number $Ma=U_1/a_s$, where a_s is the adiabatic sound speed, was kept smaller than 0.05 for all three cases, in order that deviations caused by higher order terms, terms which are similar to those aforementioned nonlinear terms in the r.h.s of the momentum equation of the nonthermal lattice BGK modeled fluid and whose effects are highly Mach number dependent, contribute only

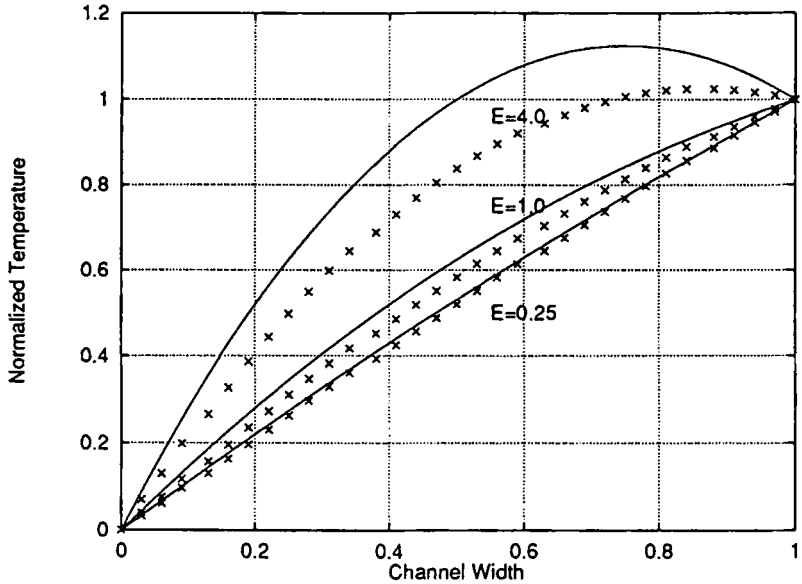

Fig. 2. Temperature profiles in Couette flows under different Eckert numbers. Solid lines are analytical solutions and crosses are the numerical results calculated by using Qian's thermal lattice BGK model.

diminishing effects in the energy transport equation. It is also clear, because of this low-Mach-number condition, that errors occurring under large Eckert number arise solely from the existence of deviation terms at least of the same order as the viscous work terms.

It becomes crucial to derive the structures of the hidden terms in the energy equation of the modeled fluid, since one may then disclose the source of the errors and improve the quality of lower order modeling if possible. In particular, the structures of these terms were derived under two optional constraints,

$$\sum_{pk} \psi_{pk} g_{pk0} = 0, \qquad \sum_{pk} \psi_{pk} g_{pk1} = 0 \tag{16}$$

$$\sum_{pk} \Lambda_{pk} j_{pk0} = 0, \qquad \sum_{pk} \Lambda_{pk} j_{pk1} = 0 \tag{17}$$

As stated above, these optional constraints were used to eliminate the influence of the higher rank anisotropic parts. Then the hidden terms may be explicitly written out in five parts,[12]

$$
\begin{aligned}
&\text{Part 1:}\quad \frac{1}{2}\partial_\alpha(\rho u^2 u_\alpha) \\
&\text{Part 2:}\quad \partial_\alpha[(\xi_1+\xi_2\delta_{\alpha\beta})\,\partial_\beta(\rho e u_\alpha u_\beta)+(\xi_3+\xi_4\delta_{\alpha\beta})\,\partial_\beta(\rho u_\alpha u_\beta)] \\
&\text{Part 3:}\quad -\partial_\alpha\left\{\left[\mu(\partial_\alpha u_\beta+\partial_\beta u_\alpha+\partial_\gamma u_\gamma\delta_{\alpha\beta})\right.\right. \\
&\qquad\left.\left.+\sigma\left(1-\frac{D-2}{2D}\delta_{\alpha\beta}\right)\partial_\gamma(\rho u_\alpha u_\beta u_\gamma)\right]u_\beta\right\} \\
&\text{Part 4:}\quad \partial_\alpha\{\zeta_1\partial_\beta[\Delta^{[4,2]}\partial_\beta(\rho u_\delta u_\zeta)]+\zeta_2\partial_\beta[\Delta^{[4,2]}\partial_\beta(\rho e u_\delta u_\zeta)]\} \\
&\text{Part 5:}\quad \sigma\left(1-\frac{1}{D}\delta_{\alpha\beta}\right)\partial_\gamma(\rho u_\alpha u_\beta u_\gamma)\,\partial_\alpha u_\beta
\end{aligned}
\tag{18}
$$

Here, $\Delta^{[4,2]}$ is used to represent the sum of permuting products of the Kronecker tensors, which has been written as $(\delta_{\alpha\beta}\Upsilon_{\gamma\delta\zeta\xi}+\ldots)$ in Eq.(4). The nonlinear response coefficients are defined by

$$
\begin{aligned}
\delta &= -\left(\tau-\frac{1}{2}\right) \\
\xi_1 &= \left[(D+4)\left(\sum_{pk}\theta_{pk}j_{pk1}\right)-\frac{D+2}{D}\right]\left(\tau-\frac{1}{2}\right) \\
\xi_2 &= \frac{1}{2}\left[(D+2)\left(\sum_{pk}\varphi_{pk}g_{pk1}\right)+(D+4)\left(\sum_{pk}\theta_{pk}j_{pk1}\right)\right]\left(\tau-\frac{1}{2}\right) \\
\xi_3 &= (D+4)\left(\sum_{pk}\theta_{pk}j_{pk0}\right)\left(\tau-\frac{1}{2}\right) \\
\xi_4 &= \frac{1}{2}\left[(D+2)\left(\sum_{pk}\varphi_{pk}g_{pk0}\right)+(D+4)\left(\sum_{pk}\theta_{pk}j_{pk0}\right)\right]\left(\tau-\frac{1}{2}\right) \\
\zeta_1 &= \frac{1}{2}\left(\sum_{pk}\Omega_{pk}j_{pk0}\right)\left(\tau-\frac{1}{2}\right) \\
\zeta_2 &= \frac{1}{2}\left(\sum_{pk}\Omega_{pk}j_{pk1}\right)\left(\tau-\frac{1}{2}\right)
\end{aligned}
\tag{19}
$$

As the definitions of ζ_1 and ζ_2 involve Ω_{pk}, the contribution of part 4 would be anisotropic. It is obvious that there exist terms of ∂u^2 order in parts 2 and 3, which result from the higher order structures of the Euler-level energy and the Navier–Stokes-level momentum equations. Since these terms are of the same order as the normal term for viscous work in the energy equation, their combined effects could be the main contributions to errors under large Eckert number. Such errors, as discussed so far, will be

less relevant to the Mach number, because none of the higher order terms in parts 1 and 5, which do bear the Mach number dependence, contribute, significantly when this dimensionless number is set low.

3.3. Results of a Revised Lower Order Model (2D13VC)

The quality of the lower order thermal lattice BGK model may be improved by making changes in the optional constraints stated in the previous section. Actually, one may relax one such constraint, Eq. (17), and impose two new constraints as follows:

$$\sum_{pk} \varphi_{pk} g_{pk0} = 0, \qquad \sum_{pk} \varphi_{pk} g_{pk1} = -\frac{1}{D} \tag{20}$$

$$\sum_{pk} \Theta_{pk} j_{pk0} = 0, \qquad \sum_{pk} \Theta_{pk} j_{pk1} = \frac{1}{D} \tag{21}$$

Note that the satisfaction of Eq. (16) can still be ensured if the stationary particles, which reside in the 00 sublattice, are included. This actually is the case for the two dimensional, 13-link thermal lattice BGK models used in the current situation.

With the use of the definition of the shear viscosity in Eq. (11), it can be shown that Eqs. (20) and (21) will lead to the cancellation of terms of $\partial^2 u^2$ order in parts 2 and 3 of Eqs. (18). The residual pertaining to heat conduction is proportional to $u^2 \partial^2 (\rho e)$, which should be vanishingly small in the low-speed limit. Nevertheless, the relaxation of Eq. (17) will bring about an additional part of the anisotropic errors, which involves the lattice-symmetric parameter Λ_{pk} and the higher order Kronecker tensor $\Upsilon_{\alpha\beta\gamma\delta\zeta\xi}$. Note that no anisotropic errors would occur in the 2D13VQ model, because Ω_{pk} is zero in the two-dimensional space and Eq. (17) obviates another contribution. As Λ_{pk} is a nonzero parameter in all the dimensions, the relaxation of Eq. (17) will certainly let one part of the anisotropic error play its role in the numerical calculation with the use of the revised lower order model.

The satisfaction of Eq. (21) may not be realized, however, without a further consideration of the lattice geometry. Since 00, 11, 12, and 21 sublattices are employed in the 2D13VQ model (refer to Fig. 3), Θ_{21} is the only nonzero parameter for the determination of the sixth-rank velocity-moment tensor in the current space dimension, and so is the φ_{21} for the fourth-rank tensor. Now that j_{210} and j_{211} would have already been decided by the φ_{pk} constraints, there would be no room for them to satisfy those Θ_{pk} constraints appearing in Eq. (21). The solution is to replace the 11 or 12 sublattice with the 22 sublattice. Parameters such as Θ_{21}, Θ_{22} and φ_{21},

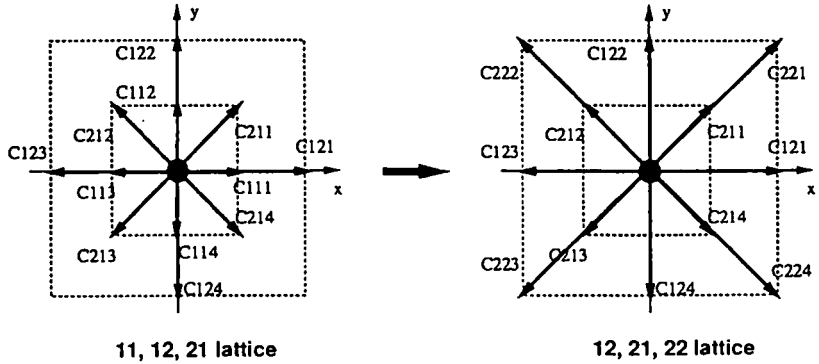

Fig. 3. Change of the underlying lattice in the revised lower order model. The 2D13VQ model uses 00, 11, 12, and 21 sublattices and the 2D13VC model uses 00, 12, 21, and 22 sublattices.

φ_{22} have nonzero values, so that the satisfaction of both the φ_{pk} and Θ_{pk} constraints becomes possible. In this investigation, 00, 12, 21, 22 sublattices are employed for the 2D13VC model, as shown in Fig. 3, to take care of the balance among particle distributions on different sublattices. With this balance, the numerical stability may be better ensured. To explain the reason in a intuitive sense, one may assume that the 11 sublattice is used instead. Now if e and u are very small on a lattice site, most of the particle density there will be naturally distributed on the 11 lattice because of the small moduli of its link vectors, which indicates low flight velocities for the particles. On the other hand, distributions of particle density on 22 would get nearly depleted. In that case, even a very small fluctuation could cause the appearance of negative particle distributions on this sublattice. Negative particle distributions will be scattered rapidly by particle propagations, and the numerical instability can be eventually triggered in the calculation; see the discussion in ref. 16.

Calculations with the revised lower order model were performed under the same conditions described above. Results for the 2D13VC model and the analytical solutions are compared with each other in Fig. 4. It is found that errors are greatly reduced even when the Eckert number reaches infinity. The remaining errors can be recognized as having two parts. The first part is brought by terms of u^3 or higher order. These errors become obvious when the Mach number is too large; see the broken line in Fig. 4. The loss of the symmetry for this line is due to the different local Mach numbers distributed across the section. Another part of the error comes from the aforementioned anisotropic terms. The behavior of these errors is an oscillating one, but small in magnitude. It is known that even the

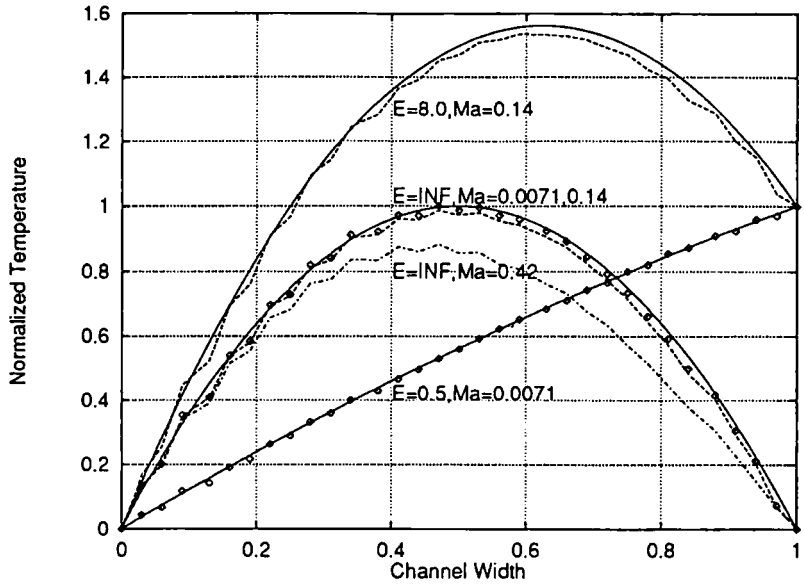

Fig. 4. Temperature profiles in Couette flows obtained by using the revised lower order thermal lattice BGK models. Solid lines are analytical solutions, others are the results of numerical calculations.

anisotropic errors can be completely deleted if both the 11 and 12 sublattices are employed in the 2D13VC model. But this could make the lower order model cost the same amount of the computer resource as the higher order model does, which is absolutely unfavorable, especially for the three-dimensional case where the lower order model could save nearly half[13] of the computer memory consumed by the higher order one.

3.4. Results of the Higher Order Model (2D16V)

It is clear that the lower order thermal lattice BGK models suffer from different errors under different conditions. Although they are improvable, errors cannot be completely avoided. On the other hand, the higher order model was designed to eliminate all these deviations. Here, only the calculation for the case of the infinite Eckert number, which was the most severe condition for the lower order models, is presented. No errors caused by the spurious viscous work or anisotropic terms can be observed in the results. Also, from the comparison of the numerical and analytical solutions shown in Fig. 5, the parabolic temperature profiles are kept well even in the transonic regime, showing that the higher order

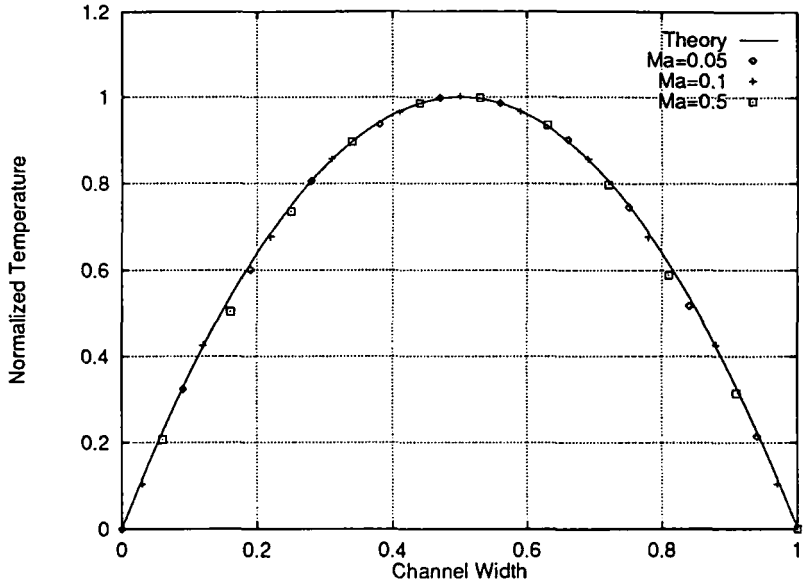

Fig. 5. Temperature profiles in Couette flows obtained by using the higher order lattice BGK model. The solid line is the analytical solution and various symbols are numerical results under different Mach numbers.

thermal lattice BGK model behaves well no matter how the Eckert or the Mach numbers change. Nevertheless, the Mach number cannot be so large as to violate the prerequisite low-flow-speed and small-Knudsen-number ($\sim$Ma/Re) limits. It was proved[13] that the deviation terms in the macroscopic momentum equation were removed for the higher order model. The calculation carried out here further demonstrates that the modeling of heat transfer by using such a model is also advantageous.

4. CONCLUDING REMARKS

Through the theoretical and numerical work presented above, the behavior of the lattice BGK modeled fluid is shown to be much the same as in Navier–Stokes fluids. Nevertheless, such an agreement can only be achieved under the condition that various limitations in the hydrodynamic derivation were kept. To apply such models to the simulation of engineering flows is impractical at this moment. The unchangeable lattice resolution, the confined flow speed, and the rather restrictive range for the temperature variation, which are inherent properties of such models, prevent them from being used to simulate high-Reynolds-number or high-

Rayleigh-number flows with appropriate numerical efficiency compared with that of conventional macroscopic and continuous methods. However, lattice BGK modeled fluids may be utilized to describe flows on rather small scales but of complicated nature, such as flows with momentum and heat transport in porous media. Before such applications can be realized, the validation of the model, especially in three-dimensional space, is absolutely necessary. This study provides some advice for the future explorations and validation for these models: If one wants to save computer resources, especially in three-dimensional situations, and does not care much about small-scale anisotropic errors, it is safe to use the revised lower order thermal lattice BGK models in the incompressible regime. On the other hand, if high accuracy is required, then the higher order model is preferable. When flows enter the transonic regime, it is essential to use the higher order model, to avoid large deviations in the simulation results.

REFERENCES

1. U. Frisch, B. Hassalacher, and Y. Pomeau, Lattice-gas automata for the Navier–Stokes equation, *Phys. Rev. Lett.* **56**(14):1505–1508 (1986).
2. G. McNamara and G. Zanetti, Use of the Boltzmann equation to simulate lattice-gas automata, *Phys. Rev. Lett.* **61**(20):2332–2335 (1988).
3. S. Chen, H. Chen, D. Martinez, and W. Matthaeus, Lattice Boltzmann model for simulation of Magnetohydrodynamics, *Phys. Rev. Lett.* **67**(27):3776–3779 (1991).
4. Y. H. Qian, D. d'Humières, and P. Lallemand, Lattice BGK models for Navier–Stokes equation, *Europhys. Lett.* **17**(6):479–484 (1992).
5. H. Chen, S. Chen and W. H. Matthaeus, Recovery of Navier–Stokes equations using a lattice-gas Boltzmann method, *Phys. Rev. A* **45**(8):R5339-42 (1992).
6. P. Bhatnagar, E. P. Gross, and M. K. Krook, A model for collision process in gases. I. Small amplitude processes in charged and neutral one-component system, *Phys. Rev.* **94**:511 (1954).
7. S. Chen, Z. Wang, X. Shan, and G. D. Doolen, Lattice Boltzmann computational fluid dynamics, *J. Stat. Phys.* **68**:379 (1992).
8. D. Martinez, W. H. Matthaeus, and S. Chen, Comparison of spectral method and lattice Boltzmann simulations of two-dimensional hydrodynamics, *Phys. Fluids* **6**(3):1285–1298 (1993).
9. S. Hou, Z. Qisu, S. Chen, G. Doolen, and A. C. Cogley, Simulation of cavity flow by the lattice Boltzmann method, preprint.
10. F. J. Alexander, S. Chen, and J. D. Sterling, Lattice Boltzmann thermohydrodynamics, *Phys. Rev. E* **47**:2249–2252 (1991).
11. Y. H. Qian and S. A. Orszag, Simulating thermohydrodynamics with lattice BGK models, *J. Sci. Comp.* **8**(3):231–242 (1993).
12. Y. Chen, Lattice Bhatnagar–Gross–Krook method for fluid dynamics: Compressible, thermal and multi-phase models, *Doctoral Thesis* (1994).
13. Y. Chen, H. Ohashi, and M. Akiyama, Thermal lattice Bhatnagar–Gross–Krook model without nonlinear deviations in macro-dynamic equations, *Phys. Rev. E* **50**:2776–2783 (1994).

14. S. Wolfram, Cellular automaton fluids 1: Basic theory, *J. Stat. Phys.* **45**:471–526 (1986).
15. G. McNamara and B. Alder, Analysis of the lattice Boltzmann treatment of hydrodynamics, *Physica A* **194**:218–228 (1993).
16. R. Benzi, S. Succi, and M. Vergassola, The lattice Boltzmann equation: Theory and applications, *Phys. Rep.* **222**(3):145–197 (1992).